International Journal of Materials Science and Applications
2017; 6(5): 241-249
http://www.sciencepublishinggroup.com/j/ijmsa
doi: 10.11648/j.ijmsa.20170605.13
ISSN: 2327-2635 (Print); ISSN: 2327-2643 (Online)

Effect of Chill Wheel Cooling on Magnetic Properties of $Nd_{15}Fe_{77}B_8$ Alloy Powders Produced by Melt Spinning Method

Sultan Öztürk[1], Kürşat Icin[1], Bülent Öztürk[1], Uğur Topal[2], Hülya Kaftelen Odabaşi[3]

[1]Department of Metallurgy and Materials Engineering, Faculty of Engineering, Karadeniz Technical University, Trabzon, Turkey

[2]TUBİTAK, National Metrology Institute Kocaeli, Gebze, Turkey

[3]Department of Airframe and Powerplant, School of Aviation Fırat University, Elazig, Turkey

Email address:

kursaticin@ktu.edu.tr (K. Icin)

To cite this article:

Sultan Öztürk, Kürşat Icin, Bülent Öztürk, Uğur Topal, Hülya Kaftelen Odabaşi. Effect of Chill Wheel Cooling on Magnetic Properties of $Nd_{15}Fe_{77}B_8$ Alloy Powders Produced by Melt Spinning Method. *International Journal of Materials Science and Applications*. Vol. 6, No. 5, 2017, pp. 241-249. doi: 10.11648/j.ijmsa.20170605.13

Received: August 14, 2017; **Accepted**: August 25, 2017; **Published**: September 19, 2017

Abstract: In this study, effect of wheel cooling on magnetic properties of $Nd_{15}Fe_{77}B_8$ alloy powders produced by melt spinning method has been investigated. The present method includes the cooling of the copper wheel by externally contacting a coolant block which is cooled by internally circulating freon gas. Within this framework, the effect of wheel temperature on the microstructure and magnetic properties of $Nd_{15}Fe_{77}B_8$ powders have been investigated. The temperatures of cooling block and melt spinning wheel were measured as -15°C and -5°C, before experimental run, separately. Produced powders exhibited different morphologies depending on the powder sizes. The smallest size of powders was formed as spherical, ligamental and fiber-like morphologies. As powders get larger, the amount of spherical, ligamental and fiber-like shaped powders decreased and the length of the fibers declined. The microstructural cell sizes for 5 µm and 48 µm size powders were measured as 0.22 µm and 1.23 µm, respectively. The cooling rates of 4 µm, 28 µm and 52 µm sized powders were measured as 5.95 x 10^6 K/s, 0.85 x 10^6 K/s and 0.45 x 10^6 K/s, respectively. The Curie temperature of produced powders was 321.5°C. The coercivity value of melt-spun powders was obtained as 2.842 kOe.

Keywords: Melt Spinning, Cooled Wheel, $Nd_{15}Fe_{77}B_8$ Magnetic Alloy

1. Introduction

Hard magnetic materials have attracted considerable attention and intensive research because of their excellent hard magnetic properties. NdFeB based alloys are most widely used and best-performing permanent magnets, and they play an important role and found various applications in industry since their discovery [1-5]. The outstanding permanent magnetic properties of these materials are based on the hard ferromagnetic tetragonal $Nd_2Fe_{14}B$ phase which has a large saturation magnetization and a high anisotropy field [6-8]. Owing to the superior magnetic properties, Nd-Fe-B magnets are used in wide range of industrial applications such as servo motors, hybrid vehicles, wind turbines, industrial motors and generators, automotive applications, magnetic resonance imaging, and so on. Due to these facts, numerous studies have been made to achieve high coercivity and high energy product of Nd-Fe-B magnets to meet the industrial demands [9]. In order to attain high energy product, it is necessary to enhance the anisotropy field and coercivity. To fabricate magnets with high energy products, the volume fraction of the magnetically hard $Nd_2Fe_{14}B$ compound as matrix phase should be maximum, non-magnetic Nd-rich phase should be located at grain boundaries and magnetically soft α-iron phase should be minimum or completely removed from the structure of sintered parts [9-11]. The grain boundary Nd-rich phase is believed that it's strong effect on the coercivity of magnets. The rate of soft magnetic α-iron phase deteriorates the hard-magnetic properties of Nd-Fe-B magnets. On the other hand, experimental studies showed that the magnetic properties of Nd-Fe-B magnetic materials are strongly dependent on the

microstructure, especially grain size and phase distribution [12]. Implementing high coercivity values, small grain sizes are essential since smaller grain sizes approach that of the domain wall widths, increase the number of grain boundaries and the number of pinning sites. Smaller grain size also reduces the possibility of nucleation of reverse domains at the grain boundaries and local demagnetizing stray fields. When grain size is equal to a single magnetic domain, the reversal of magnetic domains would change from domain wall motion to the coherent rotation state. This will end up with magnetically isolation of individual grains hence large improvement of coercivity [10].

Rapid solidification is a widespread technique and has been broadly used to produce highest performance of NdFeB based permanent magnets either by rapid quenching or by undercooling [13]. In this method, thermal energy of material which include both superheat and latent heat is rapidly extracted during solidification process from liquid state at high temperatures to solid state at room temperature. Contact time of liquid metal to substrate is limited to milli-seconds and rapid extraction of heat can cause undercooling of liquid metal as high as 100°C or more prior to the starting of solidification [14].

Rapid solidification can be realized by meeting one of following criteria;

1) Implementing excessive undercooling before solidification starts
2) Implementing a high velocity during solidification;
3) Implementing a high-cooling rate during solidification.

The first condition requires supercoiling of melt material to the temperature that the latent heat is dissipated thoroughly over the solidifying volume, before being transferred to surrounding environment. The second way to obtain rapid solidification is to move solidifying material in thinner form with high velocity. Last but not least, high-cooling rate is the most widespread technique used for rapid solidification. High cooling rates enables effective removal of thermal energy in all stages of solidification. The key parameter to achieve high cooling rate is to minimize one of the dimensions of solidifying material and exposing the material to high heat extraction rates [14].

There are many kind of different rapid solidification process in the literature [15]. The most popular technique is the melt spinning process and today's, this method is standard industrial practice for producing starting NdFeB powders with high cooling rate. This method uses a rapidly rotating copper wheel as substrate, which contacts with the molten alloys, quenches the melt, and ribbon-shaped particles are formed [16, 17]. There are several factors such as wheel speed, melt superheat, melt spinning atmosphere, gap distance between nozzle and wheel surface, pressure of ejecting gas, nozzle size and shape and the temperature and cooling conditions of copper wheel that influence the cooling behavior, the structure and properties of the rapidly solidified ribbons and powders [18, 19]. Among these parameters, the wheel speed is the most cited parameter. It is well known that the processing at different wheel speeds during the melt spinning results in different ribbon thicknesses thereby affecting the cooling rate. This in turn alters the microstructure of the as-spun ribbons and influences the magnetic properties of material [20]. However, the effect of wheel temperature and cooling conditions on the microstructure and magnetic properties of produced NdFeB powders and ribbons in melt spinning process are rarely considered process parameters and have not been systematically reported. For this reason, the effect of wheel temperature and cooling conditions on the magnetic properties and Curie temperature of produced $Nd_{15}Fe_{77}B_8$ (at.%) alloy powders were performed in this study. The present method includes the cooling of the copper wheel by externally contacting a coolant block which is cooled by internally circulating freon gas. Within this framework, the effect of wheel temperature on the microstructure and magnetic properties of $Nd_{15}Fe_{77}B_8$ powders have been investigated. On the other hand, produced melt-spun powders were subjected to surfactant-assisted high energy ball milling method with a newly designed vacuum ball milling apparatus to further enhance their magnetic properties and Curie temperatures.

2. Experimental

The $Nd_{15}Fe_{77}B_8$ (at.%) alloy used in this experiment was supplied by Alfa Aesar. The experimental studies have been performed using a laboratory scale single roller stainless steel melt spinning device operating in high vacuum atmosphere (10^{-7} mbar). The 40 mm wide copper quench wheel, 270 mm in diameter, was rotated using an external AC motor and the tangential wheel speed was controlled by a digital control unit placed out of the chamber. The surface velocity of the quenching wheel was kept constant as 52 m/s. The melt spinning apparatus includes the cooling of the copper wheel by externally contacting a coolant block made of copper. The coolant block has circular shape and involves copper pipe of 8 mm diameter coiled in circular shape and coolant freon gas circulates inside the copper pipe and the coolant block is connected to a chiller unit. The temperatures of cooling block and melt spinning wheel were measured as -15°C and -5°C, before experimental run, separately. Each run was carried out by melting 30 g of the alloy in hexagonal boron nitride crucible having rectangular slit shape of 10 x 0.7 mm. The distance from the crucible end to the quench wheel is 0.8 mm before each run and this distance is short enough to ensure a stable melt-stream but long enough to avoid any physical interaction between the crucible and the melt pool. Since the rare earth metals are very reactive chemically, the process is carried out in a vacuum atmosphere. Before each run, the chamber was evacuated to pressure of 10^{-7} mbar. The alloy was inductively melted to about 1400°C (about 150°C above the equilibrium liquidus temperature). The temperature of the melt was monitored and controlled by an infrared temperature control device located near the crucible. By introduction of an overpressure into the hexagonal boron nitride crucible, the melt of the alloy was ejected through the orifice and immediately disintegrated into fine droplets ranging from 0.5 to 700 μm with different shapes depending on powder size. These droplets were undercooled and rapidly

solidified during their free fall.

The microstructure of produced powders was examined with a scanning electron microscope (SEM) of Zeiss EVO MA model. The element contents of different phases were also analyzed by using energy dispersive X-ray analyzer (EDX) attached to the SEM. Thermal analysis of the produced and milled powders was performed to determine the Curie temperature (T_c) using the differential scanning calorimeter apparatus (DSC) of Linseis PT1600 model at a heating rate of 5°C/min. Heating was carried out with flowing purified argon gas (99.999% purity) during the DSC analysis. The magnetic properties of powders were measured with a vibrating sample magnetometer of LDJ Electronics 9600 model using a maximum applied field of 1.5 T at a room temperature.

Produced $Nd_{15}Fe_{77}B_8$ alloy powders were subjected to surfactant-assisted ball milling in a high-energy planetary ball-mill of Fritsch Pulverisette 6 model at a rotational speed of 300 rpm. A milling jar with the capacity of 250 ml performing under vacuum of 10^{-3} mbar was newly designed and manufactured from tool steel and the surface of the jar was hardened with boron-carbide material (Figure 1). The milling of melt-spun powders was performed in a protective surfactant-assisted atmosphere with the ball-to-powder weight ratio of 10/1 for milling times of 90, 150, 210, 270, 330, and 390 minutes and tungsten carbide balls of 5 mm diameter were used. Oleic acid with the purity of 99.99% was introduced in the mill as surfactant-assisted agent together with hexane and heptane (99.99% purity) as solvents. The starting materials such as powders, surfactant-assisted material, solvents and balls were charged to the jar and the jar was vacuumed to 10^{-3} mbar in the milling process. After milling operation, the slurry mixture was subjected to a size selection process including washing with hexane and removing of hexane with centrifugation cycles. The final product was dried in a glove box under argon gas atmosphere (99.999% purity). The properties of the milled materials such as morphology, chemical composition, Curie temperature and magnetism were studied in terms of milling time.

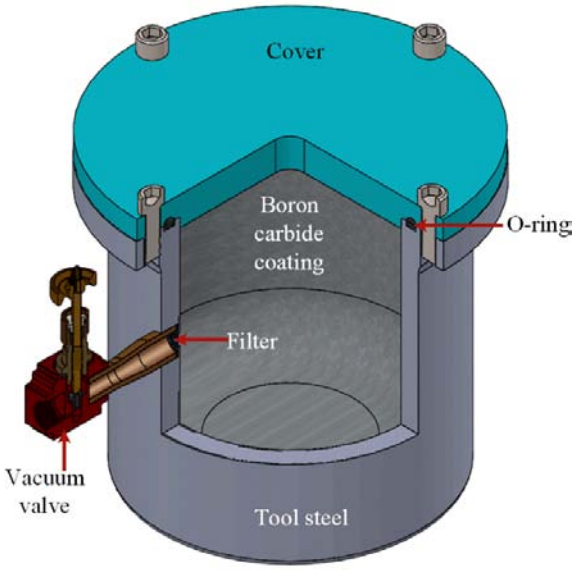

Figure 1. *Vacuum milling jar with a capacity of 250 ml.*

3. Result and Discussion

Figure 2 shows SEM morphologies of powders produced with production parameters of 52 m/s constant wheel speed, 0.5 bar argon gas pressure to eject liquid metal, 0.8 mm crucible end-wheel surface distance, and 1400°C liquid metal temperature. As illustrated in the figure, the powders exhibited different morphologies depending on the powder sizes. The smallest size of powders was formed as spherical, ligamental and fiber-like morphologies. As powders get larger, the amount of spherical, ligamental and fiber-like shaped powders decreased and the length of the fibers declined. The size of spherical particles varied from 10 µm to 25 µm. The thickness and length of the fiber-like powders changed between 10-20 µm and 100-1400 µm, respectively. The flaky shaped powders have 25-100 µm width and 80-600 µm length. The thickness of these particles varied between 10-45 µm [21, 22].

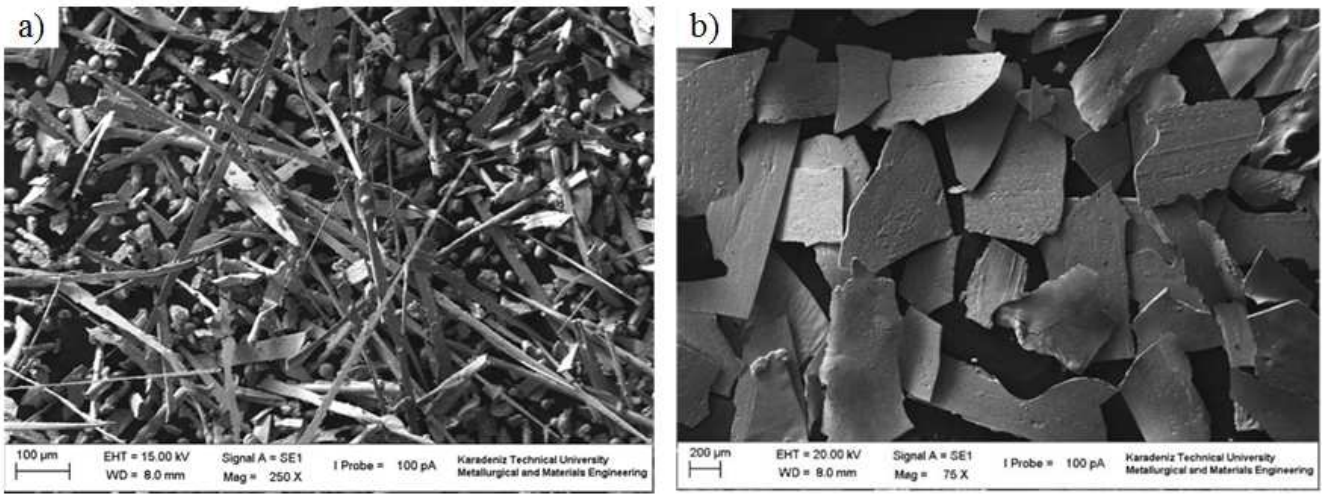

Figure 2. *The morphology of produced melt-spun $Nd_{15}Fe_{77}B_8$ alloy powders. (a) Sieve fraction is -25 µm/pan, (b) sieve fraction is -355/+250 µm.*

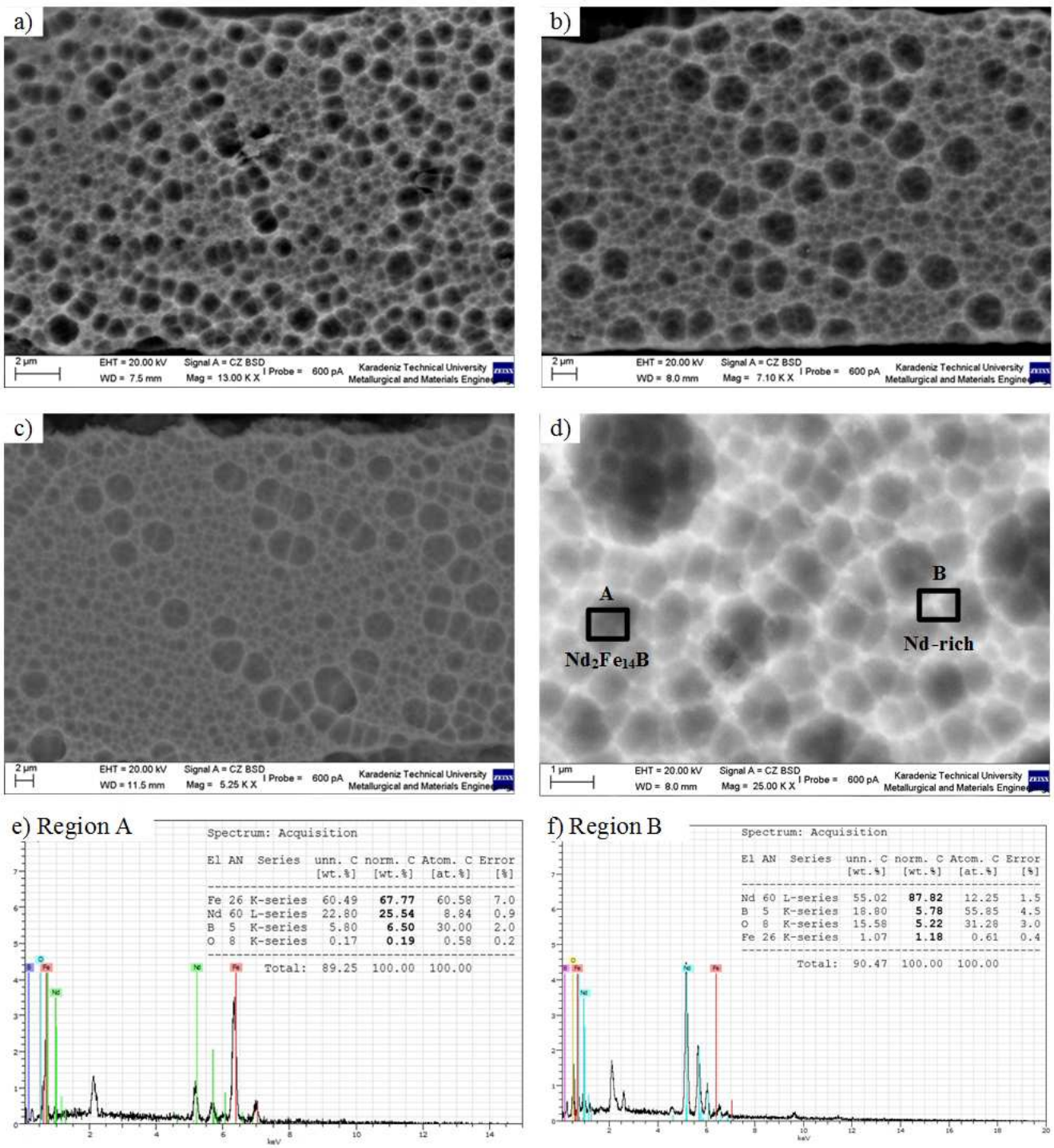

Figure 3. *(a), (b), (c), Microstructure of flaky shaped powder; the thickness of powder cross sections are 15, 25, 40 µm. (d) Detailed microstructure of $Nd_{15}Fe_{77}B_8$ alloy powders. (e) and (f) EDX analysis of produced melt-spun $Nd_{15}Fe_{77}B_8$ alloy powders. (e) Grain interior, (f) grain boundary.*

In melt spinning system, the distance of crucible end wheel surface is so small (0.8 mm) that causes the copper wheel heating during powder production process. Excess heating of copper wheel reduces the cooling rate of powders and the powder microstructures coarsen. An external coolant block made of copper, which was cooled with freon gas that circulates inside of it, was used to increase the cooling effect of the copper wheel, in this study. The temperature of copper wheel was decreased from room temperature to -5°C before experimental run. Higher cooling rates and finer grained microstructures of powders were obtained by this method. SEM microstructures of powders with increasing particle size were given in Figure 3.a-c. In these figures, the microstructures of flaky shaped particles which have 5-55 µm transversal cross section thickness were represented to compare variation of cell size with increasing particle thickness. The mean cell sizes of powders were measured with linear intercept method in

SEM studies. The mean cell sizes for 5 µm and 48 µm powders were measured as 0.22 µm and 1.23 µm, respectively. The detailed microstructure taken on the cross section of the $Nd_{15}Fe_{77}B_8$ powders is also given in Figure 3.d. As it can be seen from the figures, the microstructure was consisted of equiaxed cellular structure with most of the phases were $Nd_2Fe_{14}B$ (dark regions at grain interior) and a fine network of Nd rich phase at the grain boundaries [8, 9, 23]. The presence of these phases was easily identified by virtue of their EDX analysis and the results were given in Figure 3.e.f. By EDX analysis, it was found that $Nd_2Fe_{14}B$ phase contains 67.77 wt.% Fe, 25.54 wt.% Nd, 6.5 wt.% B and 0.16 wt.% O. The nominal composition of $Nd_2Fe_{14}B$ phase given in literature [24-26] was 72.32 wt.% Fe, 26.68 wt.% Nd and 1.00 wt.% B and the results obtained by EDX analysis correspond to values given in literature. On the other hand, the Nd-rich phase has 87.82 wt.% Nd, 5.78 wt.% B, 5.22 wt.% O and 1.18 wt.% Fe [27].

Examination of the microstructure of the flaky shaped $Nd_{15}Fe_{77}B_8$ alloy powders showed that the mean cell size of the powders decreases with the decreasing powder thickness. The mean cell sizes for 5 µm and 48 µm thick powders were measured as 0.22 µm and 1.23 µm, respectively. Some empirical equations were proposed by different authors for the estimation of cooling rates of powders. In this study, the cooling rates of powders were determined by using following equation [6, 28].

$$R = \frac{n.h.(T-T_W)}{C_p.\rho.d} \quad (1)$$

Where, R is the cooling rate, n is the form factor (1), h is the heat-transfer coefficient, T and T_w are the temperatures of the melt and copper wheel, respectively; C_p is the latent heat per unit mass, ρ is the density of the melt, and d is the thickness of the melt-spun powders. Substituting above values into equation (1), the cooling rates become 5.95 x 10^6 K/s and 0.45 x 10^6 K/s for 5 µm and 48 µm thick powders, respectively. The variations of the cooling rate and the mean cell size with the powder thickness was represented in Figure 4.

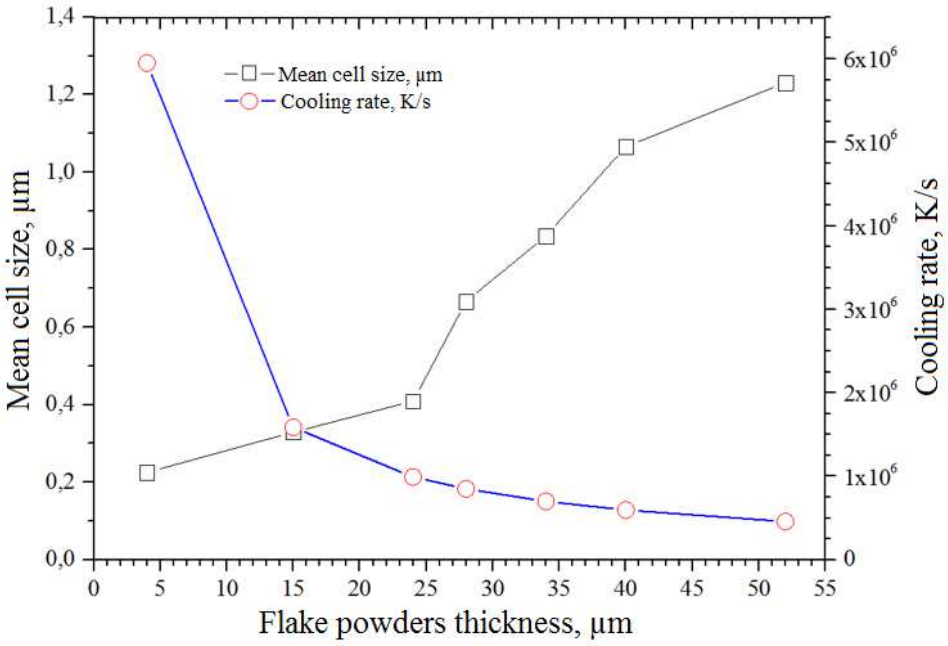

Figure 4. *Variation of cooling rate and the mean cell size with flaky shaped powder thickness.*

Melt-spun $Nd_{15}Fe_{77}B_8$ alloy powders were subjected to ball-milling process for size reduction by using newly designated vacuum jar represented in Figure 1. In this process, the powders were ball-milled with ball-to-powder weight ratio of 10/1 for milling times of 90, 150, 210, 270, 330, and 390 minutes. Oleic acid with the purity of 99.99% was introduced in the mill as surfactant-assisted agent together with hexane and heptane (99.99% purity) as solvents. Figure 5 shows the SEM micrographs of the ball-milled melt-spun $Nd_{15}Fe_{77}B_8$ alloy powders obtained for milling times of 90 and 390 minutes. It is clearly seen that with increasing milling time the size of the powders decreases significantly. The mean particle sizes of powders with milling times of 90 and 390 minutes are 1.48 µm and 0.26 µm, respectively (Figure 6). As it can be seen from Figure 5, the milled powders are agglomerated. As stated in experimental part, the slurry mixture obtained after milling was subjected to a size selection procedure which includes washing with hexane and centrifugation process. The final product was dried in a glove box under argon gas atmosphere. After drying process, the milled powders are agglomerated once again because of high surface energy and ferromagnetic character of the powders.

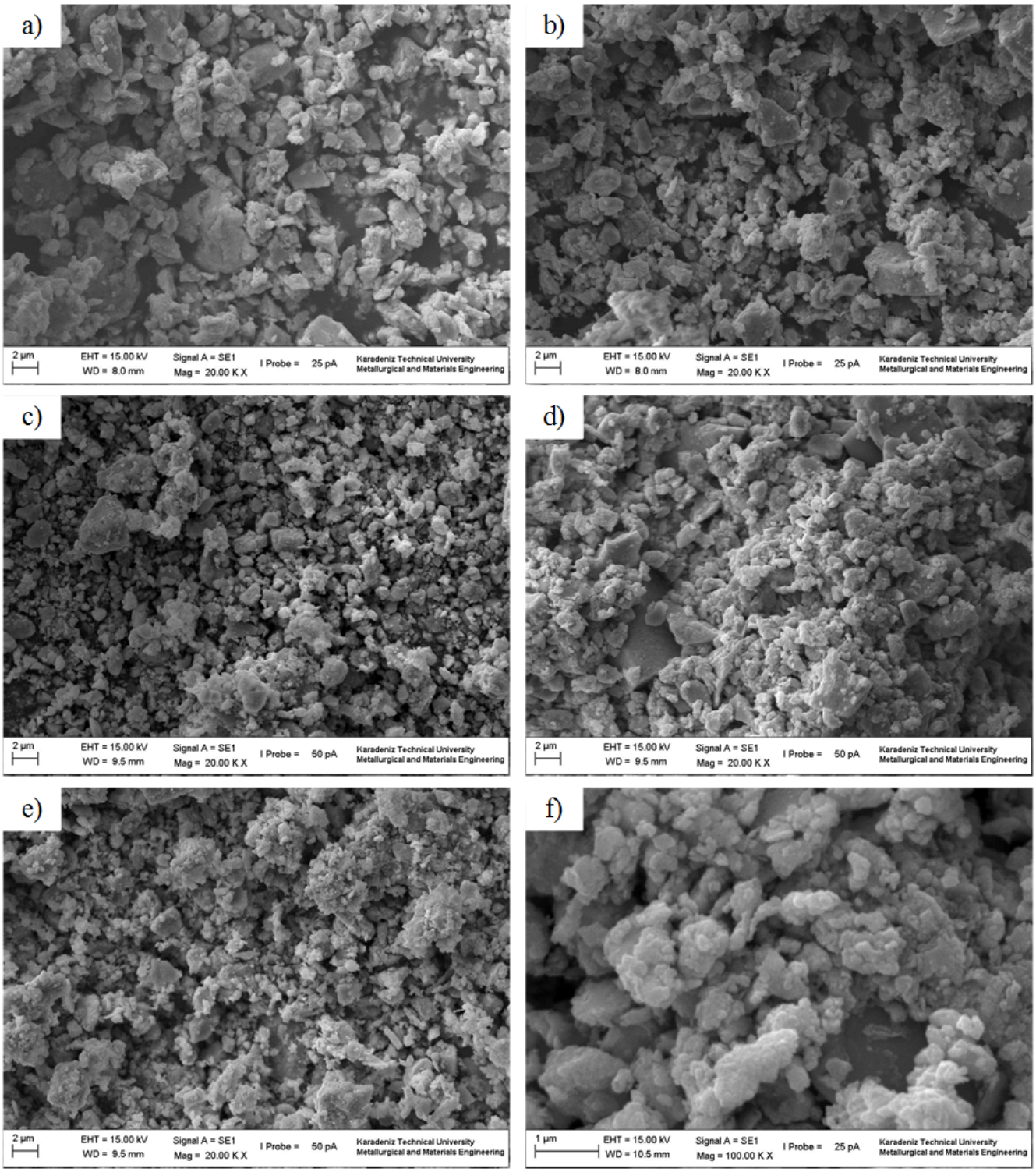

Figure 5. *SEM images of ball-milled melt-spun $Nd_{15}Fe_{77}B_8$ alloy powders. Milling time: (a) 90 min, (b) 150 min, (c) 210 min, (d) 270 min, (e) 330 min, (f) 390 min.*

The DSC curves of $Nd_{15}Fe_{77}B_8$ ingot alloy, melt-spun $Nd_{15}Fe_{77}B_8$ alloy powders and surfactant active ball-milled $Nd_{15}Fe_{77}B_8$ alloy powders with different milling time are given in Figure 7 to compare the effect of processing conditions on the Curie temperature. The DSC measurements were performed from room temperature to 600°C under protective argon gas atmosphere. It can be seen that the Curie point shifted to higher temperature from the ingot condition to surfactant active ball-milling. The Curie temperature of $Nd_{15}Fe_{77}B_8$ ingot alloy, melt-spun powders produced with cooled wheel and surfactant active ball-milled powders were obtained as 279°C, 341°C and 346°C, respectively. This increases in Curie temperature can be explained in terms of increasing amount of $Nd_2Fe_{14}B$ hard magnetic phase.

Therefore, the low amount of $N_2Fe_{14}B$ hard magnetic phase in ingot alloy causes lower Curie temperature.

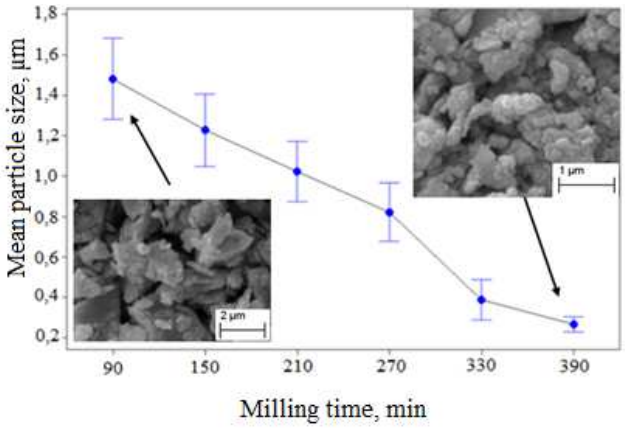

Figure 6. *Variation of mean particle size with milling time.*

Magnetic hysteresis curves were recorded for $Nd_{15}Fe_{77}B_8$ ingot alloy and melt-spun powders (Figure 8). The hysteresis curve of $Nd_{15}Fe_{77}B_8$ ingot alloy shows a constricted shape and relatively low coercivity. Such relatively narrowed shape for hysteresis curve is a sign of coexistence of hard magnetic $Nd_2Fe_{14}B$ and soft magnetic α-iron phases. The coercivity values for $Nd_{15}Fe_{77}B_8$ ingot alloy and the melt-spun powders of the same alloy are 359 Oe and 2842 Oe, respectively.

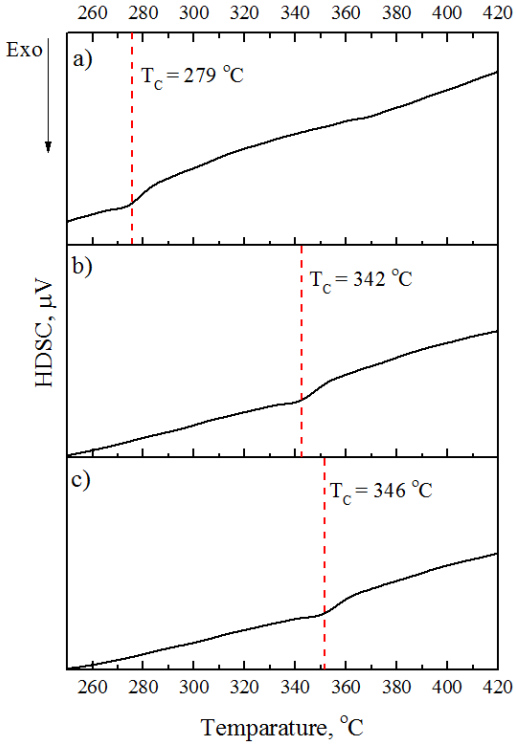

Figure 7. *DSC curves for (a) $Nd_{15}Fe_{77}B_8$ ingot alloy, (b) melt-spun powders produced with cooled wheel and (c) surfactant active ball-milled powders with 390 minutes milling time.*

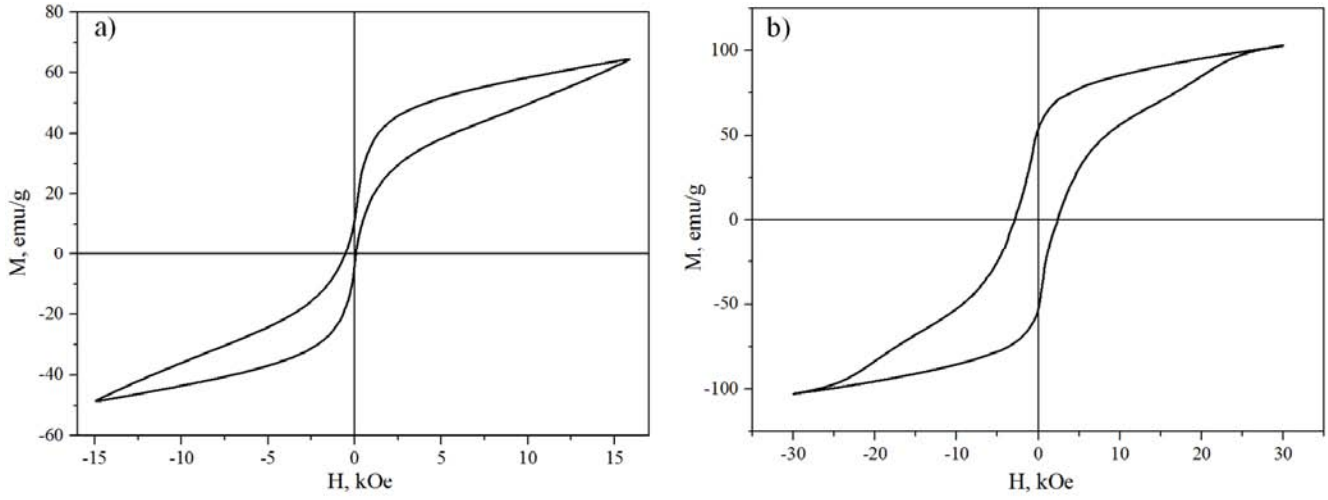

Figure 8. *Hysteresis curves for (a) $Nd_{15}Fe_{77}B_8$ ingot alloy, and (b) Melt-spun powders produced with cooled wheel.*

Figure 9 shows the effect of milling time on the magnetic properties of the melt-spun $Nd_{15}Fe_{77}B_8$ alloy powders milled for different times in a surfactant active atmosphere. The surfactant active ball milling process seems to favor the magnetic properties of melt spun $Nd_{15}Fe_{77}B_8$ alloy powders. With increasing milling time, the coercivities of powders increased significantly and the hysteresis loops get uniform shapes. All hysteresis loops exhibit a single phase-like magnetization behavior, indicating no second soft magnetic phase was present in the particles. The figure shows that the coercivity of the powders significantly increased with increasing milling time. The coercivity values for 90, 150, 210, 270, 330 and 390 min milling times were obtained as 2884, 2960, 3060, 3220, 3225, 4375 Oe, respectively, in this study.

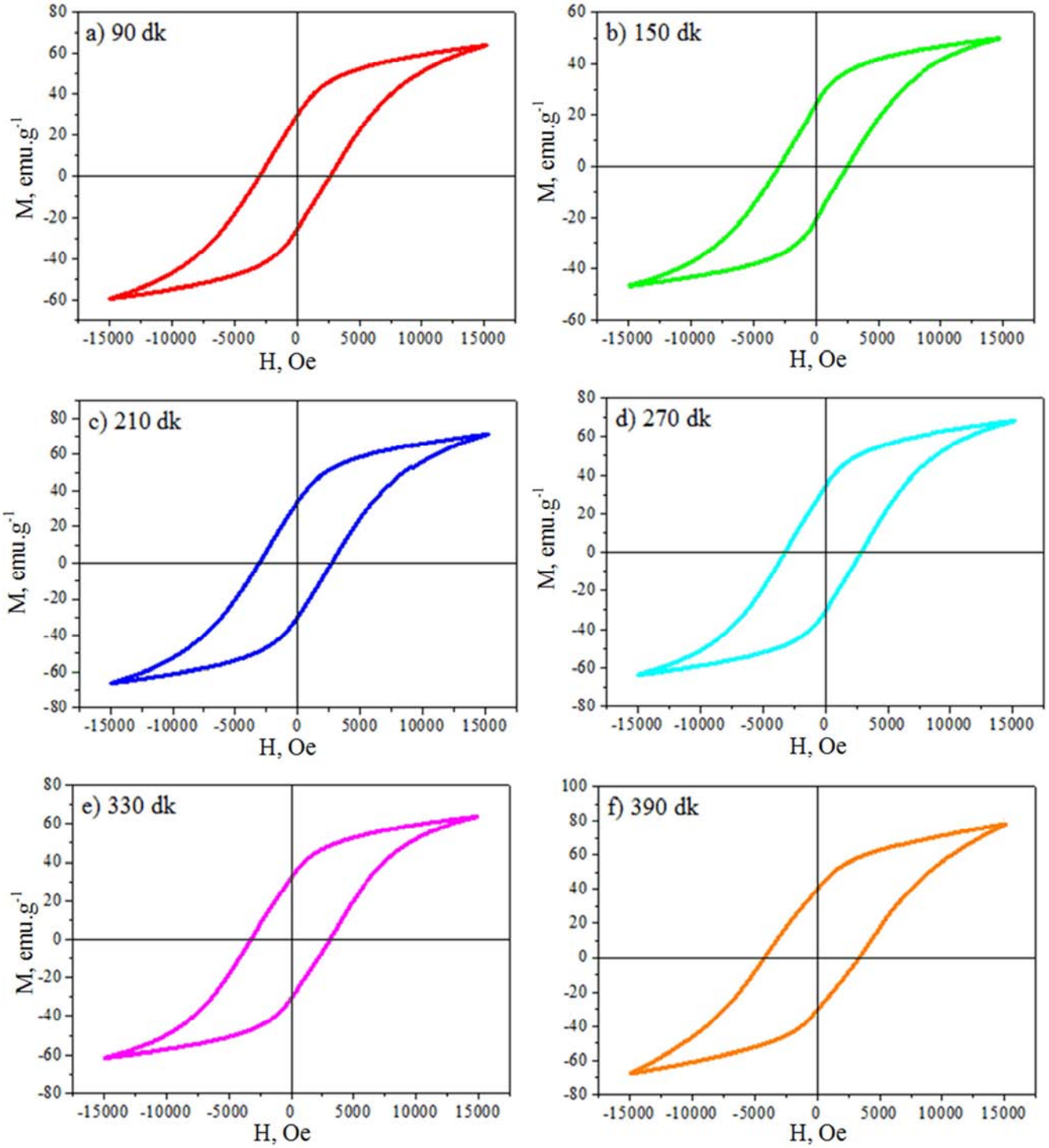

Figure 9. *Effect of milling time on the magnetic properties of the melt-spun $Nd_{15}Fe_{77}B_8$ alloy powders. Milling times: (a) 90, (b) 150, (c) 210, (d) 270, (e) 330, and (f) 390 mins.*

4. Conclusion

The important conclusions obtained from this study are listed below;

1. The mean cell sizes of produced flaky shaped powders by melt spinning method were decreased with increasing cooling rate. Therefore, the decreasing grain size has increased the coercivity of produced powder.
2. The microstructure of produced powders consisted of two phases; magnetically hard $Nd_2Fe_{14}B$ matrix phase located in grain interiors, and nonmagnetic Nd-rich phase located on grain boundaries. The fact that the hard-magnetic phase ratio is higher than the other phases has affected the Curie temperature and magnetic properties of produced powders, positively.
3. The powder size varies inversely with the milling time. The mean particle sizes of powders with milling times

of 90 and 390 minutes are 1.48 μm and 0.26 μm, respectively. Consequently, the reduction of the particle size allows the hard-magnetic phase ratio to increase with respect to the other phases, thereby improving the magnetic properties.

4. The Curie temperature of $Nd_{15}Fe_{77}B_8$ ingot alloy, melt-spun powders produced with cooled wheel and surfactant active ball-milled powders were obtained as 279°C, 341°C and 346°C, respectively. The reason for this is the increase in the cooling rate with the cooled wheel and the reduction of the particle size with the grinding time.
5. Coercivity of powders increased significantly with increasing milling time and the hysteresis loops get more uniform shape due to decreased size of the particle.

Acknowledgements

This work is supported by the scientific and technological research council of Turkey (TUBİTAK) with project number #114M501. The authors would like to thank TUBİTAK for the support.

References

[1] M. Abuin, Z. Turgut, N. Aronhime, V. Keylin, A. Leary, V. DeGeorge, J. Horwath, S. L. Semiatin, D. E. Laughlin, M. E. McHenry, Metall. Mater. Trans. A, 46 (2015) 5002-5010.

[2] B. Davies, R. Mottram, I. Harris, Mater. Chem. Phys. 67 (2001) 272-281.

[3] D. C. Jiles, Acta Mater., 51 (2003) 5907-5939.

[4] B. Ma, J. Herchenroeder, B. Smith, M. Suda, D. Brown, Z. Chen, J. Magn. Magn. Mater., 239 (2002) 418-423.

[5] Y. Matsuura, J. Magn. Magn. Mater., 303 (2006) 344-347.

[6] S. Ozawa, T. Saito, T. Motegi, J. Alloy Compd., 363 (2004) 268-275.

[7] K. Umadevi, M. Palit, J. A. Chelvane, D. A. Babu, A. P. Srivastava, S. V. Kamat, V. Jayalakshmi, J. Superconduc. Novel Magnet., 29 (2016) 2455-2460.

[8] J. Gao, T. Volkmann, S. Roth, W. Löser, D. Herlach, J. Magn. Magn. Mater., 234 (2001) 313-319.

[9] J. Gao, T. Volkmann, D. M. Herlach, J. Mater. Research, 16 (2011) 2562-2567.

[10] W. F. Li, T. Ohkubo, K. Hono, M. Sagawa, J. Magn. Magn. Mater., 321 (2009) 1100-1105.

[11] H. Sepehri-Amin, Y. Une, T. Ohkubo, K. Hono, M. Sagawa, Scripta Materialia, 65 (2011) 396-399.

[12] C. Wang, M. Yan, Mater. Sci. Eng.: B, 128 (2006) 216-219.

[13] J. Gao, B. Wei, J. Alloy Compd., 285 (1999) 229-232.

[14] E. J. Lavernia, T. S. Srivatsan, J. Mater. Sci., 45 (2009) 287-325.

[15] L. A. Jacobson, J. McKittrick, Mater. Sci. Eng. R: Reports, 11 (1994) 355-408.

[16] M. Gögebakan, O. Uzun, T. Karaaslan, M. Keskin, J. Mater. Proces. Techn., 142 (2003) 87-92.

[17] M. Kramer, L. Lewis, L. Fabietti, Y. Tang, W. Miller, K. Dennis, R. McCallum, J. Magn. Magn. Mater., 241 (2002) 144-155.

[18] S. Sarafrazian, A. Ghasemi, M. Tavoosi, J. Magn. Magn. Mater., 402 (2016) 115-123.

[19] K. Simeonidis, C. Sarafidis, E. Papastergiadis, M. Angelakeris, I. Tsiaoussis, O. Kalogirou, Intermetallics, 19 (2011) 589-595.

[20] M. Srinivas, B. Majumdar, G. Phanikumar, D. Akhtar, Metall. Mater. Trans. B: Process Metall. Mater. Proces. Sci., 42 (2011) 370-379.

[21] S. P. H. Marashi, A. Abedi, S. Kaviani, S. H. Aboutalebi, M. Rainforth, H. A. Davies, J. Phys. D: Applied Physics, 42 (2009) 115410.

[22] C. Wang, M. Yan, Mater. Sci. Eng.: B, 164 (2009) 71-75.

[23] J. Gao, T. Volkmann, D. Herlach, Acta materialia, 50 (2002) 3003-3012.

[24] X. Dong, L. He, P. Li, J. Alloy Compd., 612 (2014) 20-25.

[25] E. A. O. M. H. Saleh, F. Ismail, P. Hussain, M. Mohammad, Solid State Sci. Tech., 13 (2005) 268-275.

[26] M. Mohammed, in: Proceedings of 17th International Conference on Composite/Nano Engineering, Hawaai, USA, 2009.

[27] A. P. Jadhav, H. Ma, D. S. Kim, Y. K. Baek, C. J. Choi, Y. S. Kang, Bulletin of the Korean Chemical Society, 35 (2014) 886-890.

[28] S. Ozawa, M. Li, S. Sugiyama, I. Jimbo, S. Hirosawa, K. Kuribayashi, Mater. Sci. Eng.: A, 382 (2004) 295-300.